Case Studies in Structural Engineering 6 (2016) 84–102

Contents lists available at ScienceDirect

Case Studies in Structural Engineering

journal homepage: www.elsevier.com/locate/csse

Strut effectiveness factor for reinforced concrete deep beams under dynamic loading conditions

Ammar N. Hanoon [a,b,*], M.S. Jaafar [a], Farzad Hejazi [a], F.N.A. Abd Aziz [a]

[a] Department of Civil Engineering, Universiti Putra Malaysia, Malaysia
[b] The engineering affairs department, Baghdad University, Iraq

ARTICLE INFO

Article history:
Received 27 March 2016
Received in revised form 1 August 2016
Accepted 9 August 2016
Available online 11 August 2016

Keywords:
Deep beam
Strut effective strength
Dynamic
Strain rate
Shear strength
Strut-and-tie model

ABSTRACT

In a current study, a new strut effectiveness factor based on Strut-and-Tie Model (STM) is proposed to assess the ultimate shear strength of reinforced concrete (RC) deep beam subjected to dynamic loads. The derivation of the new effectiveness factor of concrete struts is based on Mohr–Coulomb criterion failure. Two types of concrete failure, diagonal splitting and concrete crushing failure modes, are proposed and examined. The modification of the proposed model is simulated in a MATLABSIMULINK environment. The proposed model exhibits efficiency in assessing dynamic shear resistance for deep beams. Moreover, a parametric study is then conducted to examine the effect of flexural reinforcement ratio, transverse reinforcement and shear-span to depth ratio on shear behavior of RC deep beams with consideration of the changes in strain rate. The proposed effectiveness factor is validated by utilizing the experimental results obtained from the literature and shows good accuracy for prediction the shear strength of reinforced concrete deep beams under different loading conditions.

© 2016 The Authors. Published by Elsevier Ltd. This is an open access article under the CC BY-NC-ND license (http://creativecommons.org/licenses/by-nc-nd/4.0/).

1. Introduction

During their service life, reinforced concrete (RC) structures may suffer from various deteriorations, such as cracks, concrete spalling, large deformations, and collapse [5]. Such deteriorations are caused by several factors, including aging, corrosion of steel reinforcement, and environmental effects (earthquakes, impacts, and blasts) [11,14,28].

Under high loading rates the increase in the fracture energy and peak load are influenced due to the effect of inertia force. The strength and the elastic modulus of concrete were found to increase with the increasing the loading rates. Also the yield strength and the corresponding strain of steel increased with the increasing loading rates. To get proper design for all loading types, the studying of concrete behavior under wide range of strain rate (Fig. 1) is required [22].

Numerous studies have examined the behaviors of RC slender beams subjected to drop weight impact [18,19,23] and different loading rates [3,16,17,21]. According to the current design codes, such as ACI building code [1,2,8,10,13], a RC deep beam should be analysed utilizing the STM, which takes into consideration the complex stresses flow in D-regions. Based on the best author knowledge, studies on the ultimate strength and behavior of RC deep beams subjected to different loading rates are scarce. As a result, the necessity to modify methods for assessing the deep beams ultimate shear strength has become more significant in current literature topics. Therefore, this study aims theoretically to examine the ultimate shear

* Corresponding author at: Department of Civil Engineering, Faculty of Engineering, Universiti Putra Malaysia, Malaysia.
E-mail addresses: civileng.ammar@gmail.com, structuraleng.ammar@gmail.com (A.N. Hanoon), msj@upm.my (M.S. Jaafar), farzad@fhejazi.com (F. Hejazi), farah@upm.edu.my (F.N.A.A. Aziz).

http://dx.doi.org/10.1016/j.csse.2016.08.001
2214-3998/© 2016 The Authors. Published by Elsevier Ltd. This is an open access article under the CC BY-NC-ND license (http://creativecommons.org/licenses/by-nc-nd/4.0/).

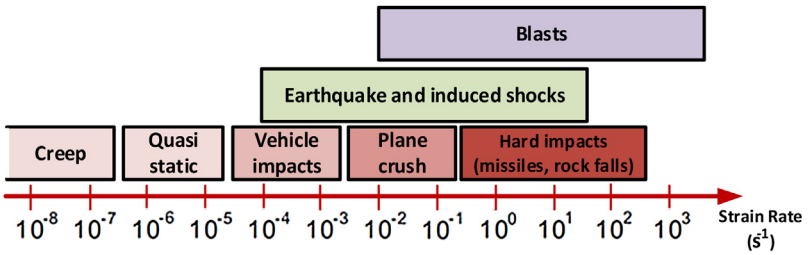

Fig. 1. Strain rate according to real loads [22].

capacity of RC deep beams under dynamic loading conditions, and suggests a new effectiveness factor which utilizes in the STM for designing of RC deep beams subjected to different loading rates. This factor plays a significant role in the STM design of RC deep beams and shear capacity prediction.

Various factors affect on the value of the effectiveness factor, for instance material properties, beam size, steel reinforcement, and structure loading. According to MacGregor et al. [20] the effectiveness factor ν differs from 0.25 to 0.85 based on the concrete strut in the plastic truss model utilized to estimate the deep beam capacity.

In the present study, the STM is extended to account for the ultimate shear strength of RC deep beams under varying loading rates. The proposed model considers the effect of the combined tensile strength of longitudinal and transverse reinforcements and the tensile strength of concrete. A linear failure criterion based on modified Mohr–Coulomb theory is adopted. A simple and refined interaction formula for predicting the ultimate dynamic shear strength of RC deep beams is derived. To imply and integrate the dynamic effect, the proposed constitutive relationships of concrete and reinforcing steel [16] are taken consideration. The proposed model considers the interaction between two failure modes, namely, diagonal splitting and concrete crushing of struts. A case study is also presented to verify the proposed method for deep beams subjected to varying loading rates. The analysis results indicated a good accuracy for prediction the ultimate shear strength of RC deep beams under dynamic loading conditions.

1.1. Research significance

Limited information has been recorded on RC deep beams subjected to dynamic loads in literature. Moreover, the previous proposed STM approaches for RC deep beams and design equations used for slender beams, are mostly over or under estimation due to it is empirical nature. A new strut effectiveness factor for deep beams under different loading rates is proposed, with a refined STM which used to assist in the appropriate design of such members.

1.2. Limitations and assumptions of the proposed model

To develop the applicability of the STM concept for RC deep beams under dynamic loads, the following assumptions and limitations are made:

- The proposed model is confined for simply supported RC deep beams.
- A uni-axial compressive stress f_2 (Fig. 1) is applied to the concrete strut which inclined at an angle q with respect to the beam axis;
- The failure of shear tension caused by the inadequate anchorage of flexural reinforcement is not considered.
- The proposed model considers the effect of crushing and diagonal splitting concrete failure.
- The proposed model implies the dynamic effect by considering the constitutive relationships of concrete and steel reinforcement which proposed by Fujikake et al. [16]
- The proposed model implies iterative procedures to calculate the ultimate strength of deep beams under dynamic loading conditions.

2. Stress–strain relationships of concrete and steel reinforcing under dynamic loading

*2.1. Material **model for concrete***

Concrete materials are sensitive to changes in strain rates. Under dynamic loading rates, both tensile and compressive concrete strengths significantly increase. In the current study, the strain effect, which can be accounted by utilizing a Dynamic Increase Factor (DIF). The DIF values proposed in the literature Fujikake et al. [16] are used for both concrete and steel materials. Fig. 2 shows the constitutive relationships for the stress–strain of concrete and steel reinforcement [16].

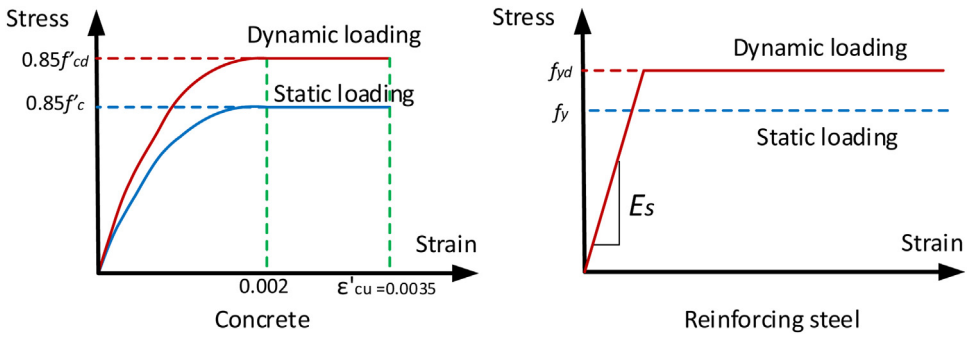

Fig. 2. Constitutive relationships of concrete and reinforcing steel.

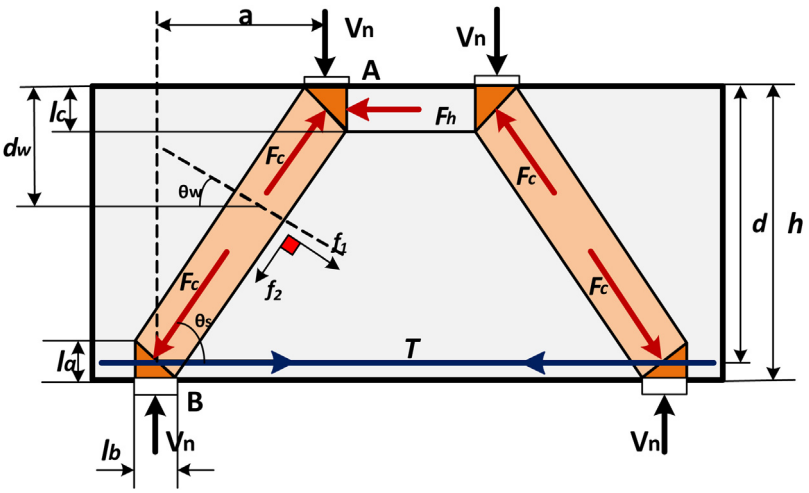

Fig. 3. Strut-and-tie model for simply supported deep beams.

For concrete in compression:

$$\mathrm{DIF} = \frac{f'_{C,\mathrm{dyn}}}{f'_C} = \left(\frac{\dot{\varepsilon}}{\dot{\varepsilon}_s}\right)^{0.006\left[\log 10\left(\frac{\dot{\varepsilon}}{\dot{\varepsilon}_s}\right)\right]^{1.05}} \tag{1}$$

Where

$f'_{C,\mathrm{dyn}}$ refers to the dynamic concrete compressive strength (MPa), $\dot{\varepsilon}$ is the strain rate, and f'_C is the static concrete compressive strength (MPa).

$$\dot{\varepsilon}_s = 1.2 \times 10^{-5}\left(\mathrm{s}^{-1}\right) \tag{2}$$

2.2. Material model for steel

For the reinforcing steel, the dynamic yield strength $f_{y,dyn}$ can be calculated from Eq. (3) [16] with consideration of the changes in strain rate $\dot{\varepsilon}$.

$$\mathrm{DIF} = \frac{f_{y,dyn}}{f_y} = (1.202 + 0.04 \log 10\dot{\varepsilon}) \geq f_y \tag{3}$$

where

f_y refers to the static yield strength of steel reinforcement.

2.3. Mechanisms of shear resistance in deep beams

By referring to Fig. 3, two stresses are created through the diagonal strut because of the applied load V_n (Fig. 3).

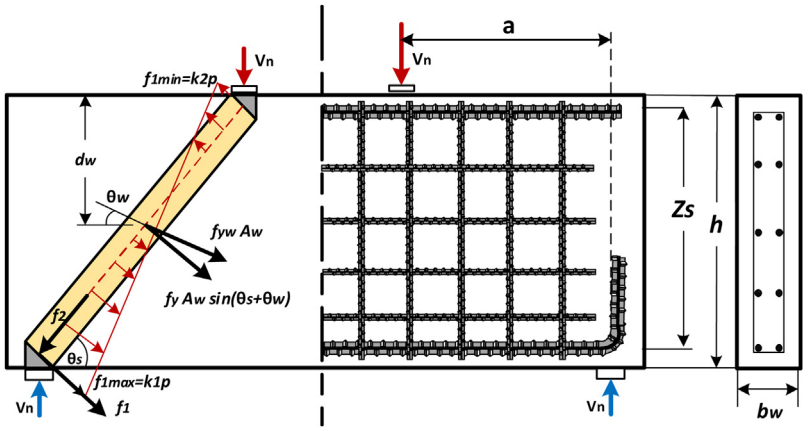

Fig. 4. Determination of Tensile Stress f_1 at Bottom Nodal Zone.

1. Compressive stress f_2 is created through a direction between t aed load and support. This stress causes the possible formation of a concrete crushing failure in the diagonal strut, which has to be resisted by the concrete compressive strength $\upsilon f'_c$ [8] (CSA, 1994).
2. Transverse tensile stress f_1 is created in a direction perpendicular to the diagonal strut. Consequently, the deep beam may fail by concrete splitting, which can be resisted by the longitudinal steel, transverse reinforcement, and concrete tensile strength.

The equilibrium forces at the bottom nodal zone (B) of the diagonal strut (Fig. 3**)** are concluded through the following

$$\sum F_y = 0; \quad F_c = \frac{V_n}{\sin\theta_s} \tag{4}$$

$$\sum F_x = 0; \quad T = \frac{V_n}{\tan\theta_s} \tag{5}$$

θ_s refers to the angle of the inclined strut and is defined by

$$\tan\theta_s = \frac{Z_s}{a} \tag{6}$$

where a is the distance between the applied load and support, and is the lever arm of the longitudinal reinforcement to the center of the upper strut (Fig. 4) and can be defined as follows.

$$Z_s = h - \frac{l_a}{2} - \frac{l_c}{2}$$

where, l_a *and* l_c are the depth of the top and bottom nodal zones, respectively (Fig. 3).

The compressive stress f_2 can be calculated from Eq. (4) as follows:

$$f_2 = \frac{F_c}{A_{str}} = \frac{V_n}{A_{str}\sin\theta_s} \tag{7}$$

where, A_{str} is the diagonal strut cross-sectional area (mm^2), and V_n is the applied load (kN).

To determine the principal tensile stress f_1 (Fig. 3) perpendicular to the diagonal strut at the bottom nodal zone, first csider a deep beam [25]

$$f_1 = \frac{kT\sin\theta_s}{A_c/\sin\theta_s} = kP \tag{8}$$

where *Ac* is the deep beam cross-sectional area; and $kT\sin\theta_s/\left(A_c/\sin\theta_s\right)$ is the average tensile stress across the diagonal strut due to the component of T in the principal tensile direction of the bottom nodal zone, $T\sin\theta_s$ (Fig. 4), and k is the stress distribution factor.

The stress distribution is nonlinear and cannot be determined directly by the assumptions of the beam theory, therefore assumptions are needed to find the stress distribution factors (k_1 and k_2), as displayed ig. here k_1 and k_2 refer to the stress distribution factors at the bottom and top nodal zones, respectively. Previous studies [24,29] found that the values of stress distribution factors k_1 *and* k_2 of 2 and 0, respectively. This indicated best agreement with experimental results of RC deep beams under static loading conditions. The bottom nodal zone experiences a biaxial tension-compression stress state, and

the compressive strength of concrete is reduced due to the softening effect of the tensile stress. Based on the modified from the Mohr-Coulomb theory [9], in this study the failure criterion at the bottom nodal zone is assumed as a linear interactive relationship between f_1 and f_2, as displayed in the next section.

2.4. Consideration of concrete softening effect

Three main approaches, which take into consideration the concrete softening effect under biaxial tension–compression, are used. These approaches are summarized in the following:

1. Many of the codes, including [1,2,6,8], adopt the concrete strength efficiency factors, thereby resulting in statistical test results. However, an argument exists in evaluating the factors. Moreover, for some specific conditions, these factors may be over- or underestimated because they are defined as empirical values.
2. Function expressions, such as $\beta = f(\varepsilon_1)$, are used to consider the influence of principal strain on the compressive strength [10,12,15]. This method seems to be more accurate, but adds complexity because of the simultaneous application of equilibrium conditions, compatibility equations, and stress–strain relationships.
3. Linear interactive failure criteria, such as modified Mohr–Coulomb theory [24], are utilized to account for the softening effect directly. Thus, the relationship of Eq. (9) is utilized in this research.

$$\frac{f_1}{f_t} + \frac{f_2}{\acute{f}_{c,dyn}} = 1 \tag{9}$$

where f_1 and f_2 = respective principal tensile and compressive stresses at the nodal zone, and they represent the actual stress state; $f'_{c,dyn}$ = cylinder compressive strength under dynamic effect, and it represents the maximum compressive capacity in the f_2 direction; and f_t = tensile strength contribution of reinforcement, and concrete, and it represents the maximum tensile capacity in the f_1 direction.

Consequently, Eq. (9) is not applicable as the bottom nodal zone experiences a biaxial compression–compression stress state. Although there is additional lateral confinement available at the bottom nodal zone, the authors suggest that the compressive stress f_2 along the diagonal strut should not exceed $f'_{c,dyn}$. Thus

$$f_2 \leq f'_{C,\mathrm{dyn}} \tag{10}$$

Furthermore, the top nodal zone also experiences a biaxial compression–compression stress state. Therefore, if the width of the top-loaded region is comparable to that of the bottom support region, Eq. (10) is sufficient to safeguard failure of the top nodal zone. Thus, no further consideration is given to the top node.

The denominator term f_t in Eq. (9) is the combined tensile strength contribution of reinforcement, and concrete and it is given by

$$f_t = \frac{kA_s f_{y,dyn} \sin\theta_s}{A_c / \sin\theta_s} + \frac{2A_w f_{yw,dyn} \sin\left(\theta_s + \theta_w\right)}{A_c / \sin\theta_s} \frac{d_w}{d} + f_{ct} \tag{11a}$$

where A_s, and A_w are respective total areas of longitudinal and web reinforcement; $f_{y,dyn}$ and $f_{yw,dyn}$, are respective yield strengths of longitudinal and web reinforcement, and f_{ct} is tensile strength of concrete and is given by

$$f_{ct} = 0.5\sqrt{f'_{C,\mathrm{dyn}}} \tag{11b}$$

The first term in Eq. (11a) represents the tensile capacity of longitudinal steel reinforcement and is derived in a similar fashion as the term f_1 in Eq. (8), except that the full strength of longitudinal reinforcement is used in place of T. Furthermore, the effect of longitudinal reinforcement ($A_s f_{y,dyn} \cos\theta_s$) in the f_2 direction has been ignored for simplicity. For a deep beam with a very small a/d ratio, this component will be insignificant, as $\cos\theta_s$ approaches zero. On the other hand, if the a/d ratio is relatively high, the deep beam is likely to fail due to excessive tensile stress in the f_1 direction. In this case, failure is governed bthe first term in Eq. (9), and thus the term has f'_c little influence on the ultimate shear strength. Therefore, it is justifiable to neglect the contribution of longitudinal reinforcement to the compressive capacity in the f_2 direction. The same assumption is made for web reinforcement.

The second term in Eq. (11a) represents the tensile capacity of inclined web reinforcement at an angle θ_w to the horizontal axis in Fig. 4. It takes account of different positions and arrangements of web reinforcement, be it vertical, horizontal, inclined, or combined. From the geometry of the strut-and-tie model, the tensile force contribution of web reinforcement in the f_1 direction is $A_w f_{yw,dyn} \sin\left(\theta_s + \theta_w\right)$. The positional influence factor d_w/d [25] is introduced to account for different levels of web reinforcement.

For simplicity, the second term in Eq. (11a) can be reduce to $\frac{A_{sv} f_{yw,dyn} \sin 2\theta_s}{2A_c}$ or $\frac{A_{sh} f_{yw,dyn} \sin^2\theta_s}{A_c}$, respectively, where A_{sv} and A_{sh} refer the total areas of vertical and horizontal web reinforcement within the distance of spear span.

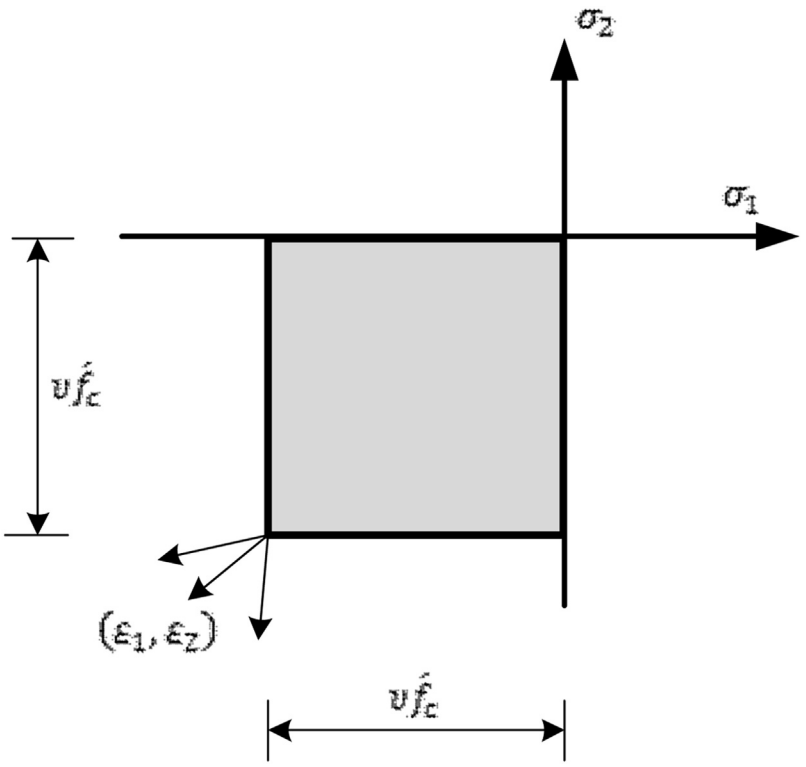

Fig. 5. Modified Coulomb Failure Criteria.

If the bottom nodal zone is subjected to the biaxial compression–compression stress state, the following equation can be derived from Eq. (10):

$$V_n \leq A_{str} f'_{C,\mathrm{dyn}} \sin\theta_s \tag{12}$$

2.5. Strut effectiveness factor derivation

Numerous analytical models [7,26,27] have been proposed to take in consideration the effect of compression softening in RC cracking for tension–compression stress states. Based on the proposed STM, the equation that yields the concrete strut effectiveness factor υ (Fig. 5) can be expressed as:

$$\frac{F_c}{A_{str}} = \upsilon f'_{C,\mathrm{dyn}} \tag{13}$$

Substituting Eqs. (7), (8) and (13) into Eq. (9), the following equation can be obtained:

$$\upsilon = \left(1 - \frac{kT_s \sin^2\theta_s}{A_c f_t}\right) \tag{14}$$

where T_s refers to the tension force in the bottom steel reinforcement and can be illustrated as $\varepsilon_s E_s A_s$. It is noteworthy that the second term in Eq. (14) represents the contribution of the tension force of the bottom steel resolved in the direction of the diagonal strut, which negates a certain amount of compression force in the strut itself. Substituting Eq. (11a) into Eq. (14) and using the relationship between T_s and ε_s, the following equation for the effectiveness factor is created,

$$\upsilon = \left(1 - \frac{k\varepsilon_s E_s A_s \sin^2\theta_s}{A_c f_t}\right) \tag{15}$$

where E_s and A_s are respectively the elastic modulus and cross sectional area of longitudinal reinforcement; ε_s is the strain in the longitudinal reinforcement; θ_s is the inclined angle of the strut.

As shown in Eq. (12) the effectiveness factor is influenced by many variables, such as concrete compressive strength steel yield strength, and steel reinforcement ratios. However, the strut angle θ_s is the main variable that affects the effectiveness factor u significantly.

The nominal shear strength V_n can be derived by substituting Eqs. (13) and (14) into Eq. (1) as follows:

$$V_n = \upsilon A_{str} f'_{C,\mathrm{dyn}} \sin\theta_s \tag{16}$$

2.6. STM dimensioning

The cross-sectional area of the strut A_{str} is calculated by the following:

$$A_{str} = b_w \left(l_a \cos\theta_s + l_b \sin\theta_s\right) \tag{17}$$

where b_w is the width of the beam, l_a is the bottom tie depth (mm), and l_b is the support-bearing plate width (mm).

T depth of the top node l_c can be determined considering the limit equilibrium of the top node. If a stress limit of $0.85f'_c$ is imposed on the top node, the depth l_c can be determined from Eq. (18).

$$l_c = \frac{V_n}{0.85f'_{C,\mathrm{dyn}} b_w \tan\theta_s}. \tag{18}$$

The l_c value cannot be calculated at first. Consequently, θ_s cannot be determined, which makes an iterative approach necessary. The value of the nominal shear strength V_n can then be calculated by utilizing Eq. (16) during the iterations. Fig. 6 displays the iterative steps to calculate the ultimate capacity of RC deep beams. A **MATLAB** simulation environmental has been used to simulate the ultimate shear strength of RC deep beams subjected to dynamic loads. At least four to five iterations are appropriate to obtain a convergence in the results.

2.7. Influence of stress distribution factor k on the prediction of ultimate strength $\boldsymbol{V_n}$

As displayed in Eq. (11a), the maximum tensile strength in the f_1 direction is:

$$f_t = \frac{kA_s f_{y,dyn} \sin\theta_s}{A_c/\sin\theta_s} + \frac{2A_w f_{yw,dyn} \sin\left(\theta_s + \theta_w\right)}{A_c/\sin\theta_s} \frac{d_w}{d} + f_{ct}.$$

where, k is the stress distribution factor, and it is assumed that the tensile stress transverse to the concrete strut is k_{pt}.

The beam ultimate shear strength can be expressed from Eq. (16)

$$V_n = \upsilon A_{str} f'_{C,\mathrm{dyn}} \sin\theta_s$$

From Eqs. (11a) and (16), it is observed that for RC deep beams without transverse reinforcement, and tensile contribution of concrete, the ultimate beam capacity is not dependent on stress distribution factor k. That leads to the shear strength V_n to be constant along the diagonal concrete strut. This occurred due to ignored the second and third part of Eq. (11a) and omitting k value. However, for optimal assessing of shear strength, the et of f_{ct}, and transverse reinforcement is taken in consideration. In order to display the influence of k on the ultimate capacity of RC deep beams, a parametric study is undertaken. With a longitudinal reinforcement rf 3.26%, and a/d of 1.0, 150 imaginary RC deep beams are examined utilizing the proposed model. In addition, a wide range of strain rates of (0.004, 0.04, 0.4, and 21/s), and concrete compressive strength of (20, 40, *and* 60*MPa*) have been used in the analysis. In this study the value of k is assumed equal to 2.5. The influence of k on the model prediction of the ultimate shear strength V_n can be expressed by $(V_n - V_{k=2.5})/V_{k=2.5}$, where $V_{k=2.5}$ represents the shear strength obtained using the proposed model with $k = 2.5$. The plotted curves are shown in Fig. 7.

For increasing the strain rates, the ultimate shear strength predicted decreases quickly with k increasing. Similarly, the ultimate shear strength decreases more quickly for higher concrete compressive strengths as increasing of k factor (Fig. 5). Generally, for $0 \le k \le 2.5$, the estimation is smaller than for $k = 2.5$, and greater when $2.5 \le k \le 10$. As displayed in Fig. 7, the reduction in the ultimate shear strength is about 5% for k greater than 2.5, thus, it can be said that $k = 2.5$ proposed is sufficiently accurate for the proposed model estimations.

As displayed in Fig. 8, the strut effectiveness factor value influenced by stress distribution factor and the strain rate values. The results indicated an increasing in the effectiveness factor with decrease in the K factor. Moreover, there is a decreasing in the strut effectiveness factor value with increase the strain rates which may be occurring due to the crack growth.

3. Comparision of test results with case study

Scarce studies have been recorded in literature for RC deep beams subjected to dynamic loads. Thus, to evaluate the proposed model, a case study [4] was employed for verification purposes. This case study dealt with RC deep beams under dynamic loading conditions.

3.1. Case study description

A total of 12 RC deep beams were tested under point loading [4]. The experimental objective was to examine the influence of loading rates on ultimate shear strength and the behavior of RC deep beams. Fig. 9 shows the notation utilized to describe

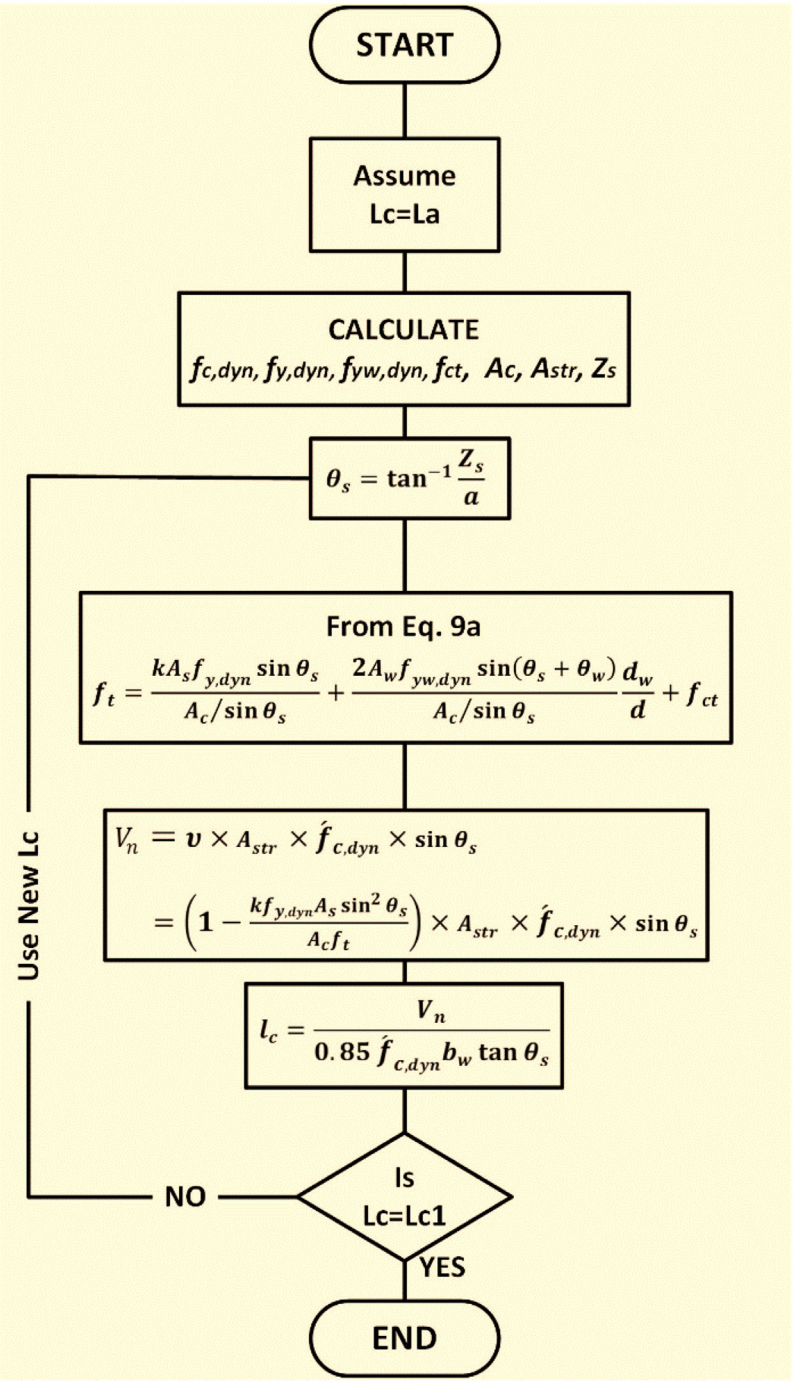

Fig. 6. Iteration steps for calculating the ultimate strength.

the test parameters of each specimen and the relevant details. All the beam specimens had an overall depth of h = 250mm with an effective depth and beam width of d = 210mm and b_w = 150mm, respectively (Fig. 6). The beam specimens comprised two ϕ22mm bars as flexural reinforcement at top and bottom, whereas ϕ6mm deformed bars were utilized as web reinforcements. The yield strength of longitudinal and web reinforcement are f_y = 371MPa, and $f_{yv} = f_{yh}$ = 442MPa, respectively. Table 1 describes the ultimate capacities of the RC deep beams according to the test results, and Fig. 10 presents the specimen designations.

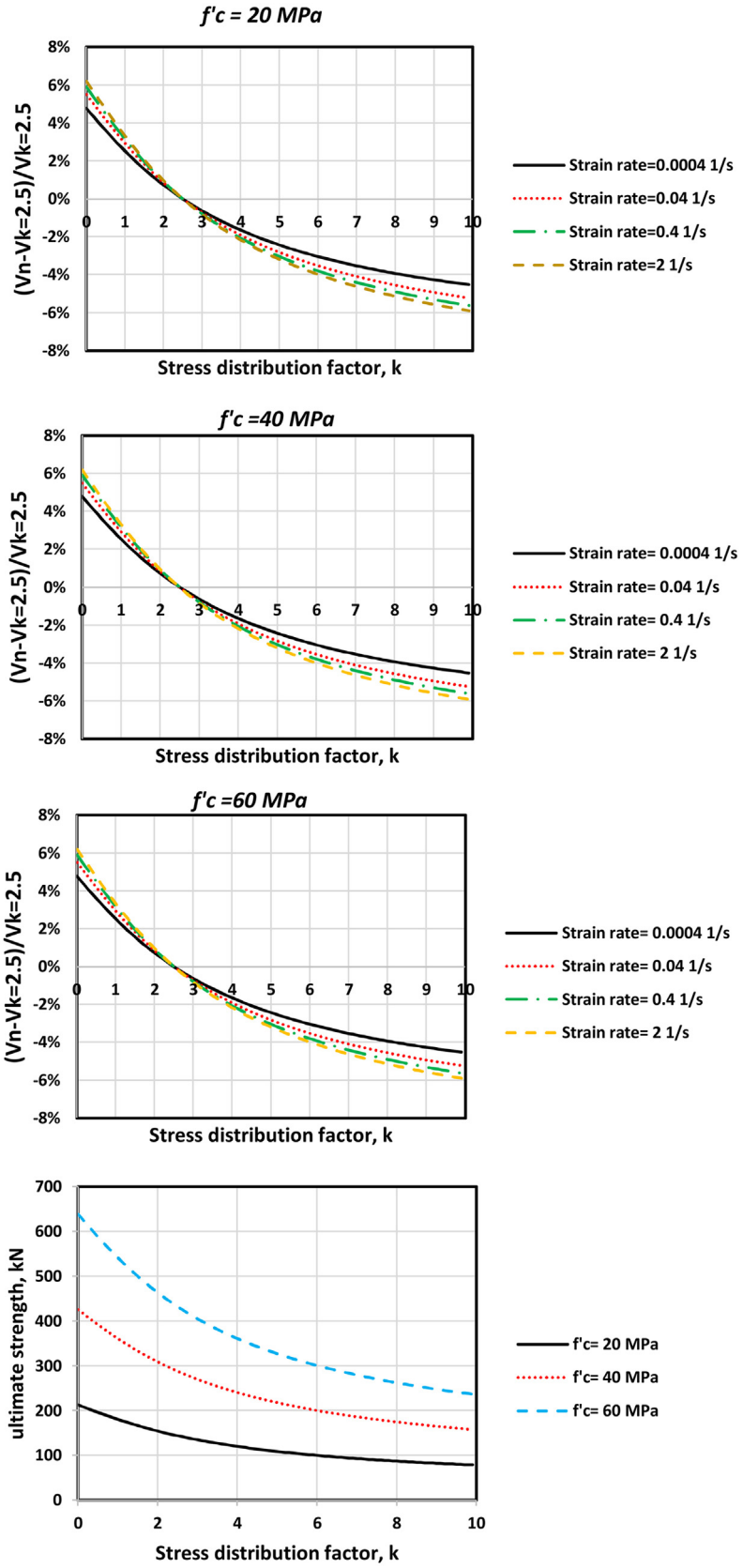

Fig. 7. Influence of stress distribution factor k on the ultimate shear capacity estimations.

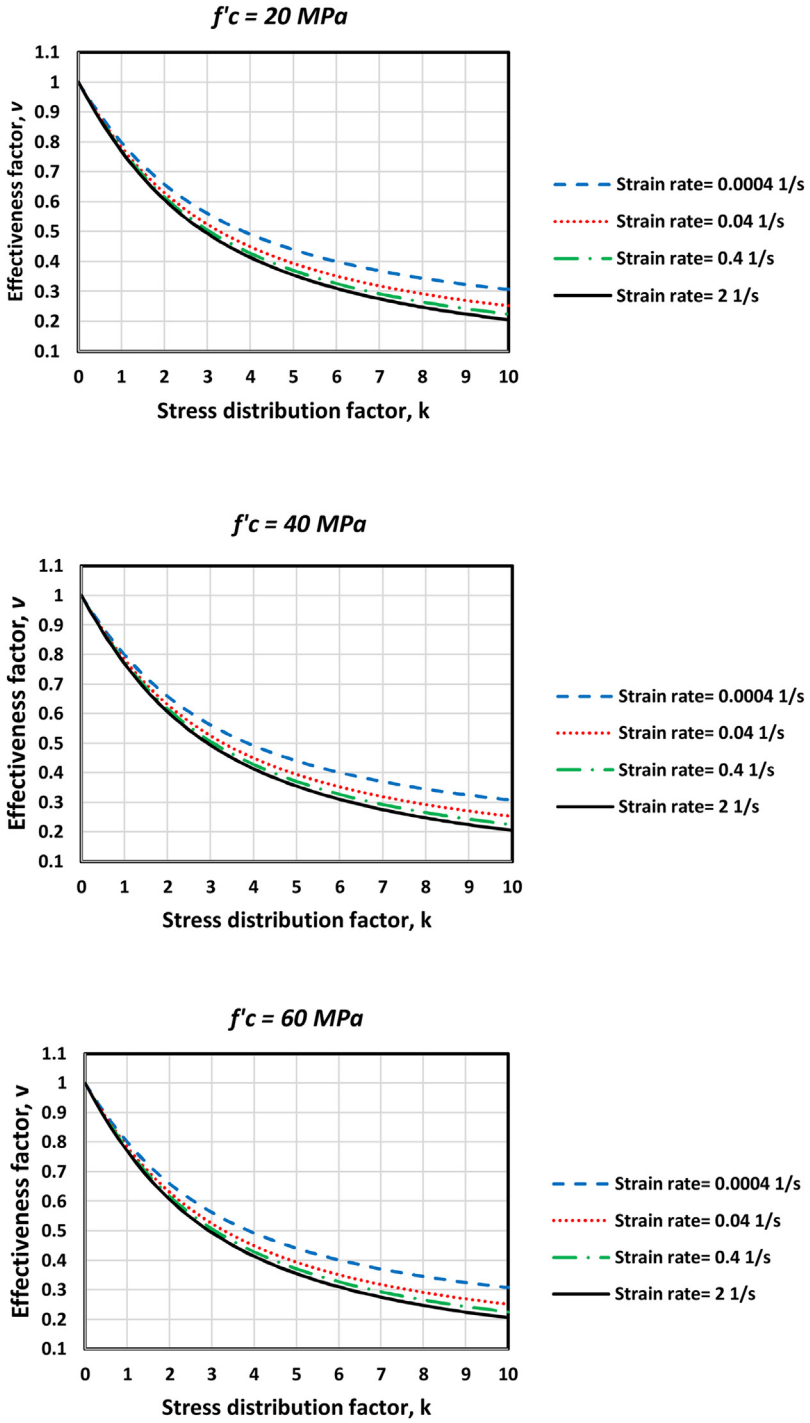

Fig. 8. Influence of stress distribution factor, k on the strut effectiveness factor prediction.

4. Results discussion

Table 2 demonstrates the statistical analysis of the ultimate strengths predicted by the proposed model once again match the experimental results well. The mean value of the prediction is 0.976 with a standard deviation of 0.172 and coefficient of variation of 0.176. Figs. 11 and 12 display the comparison of model predictions with the experiment performed in Adhikary et al. [4]. There is only one beam (Table 2) that has inaccurate prediction. This indicates that the proposed STM model is generally trustworthy. It is also remarkable that the mean value of the case study is very close to 1.0 (0.976).

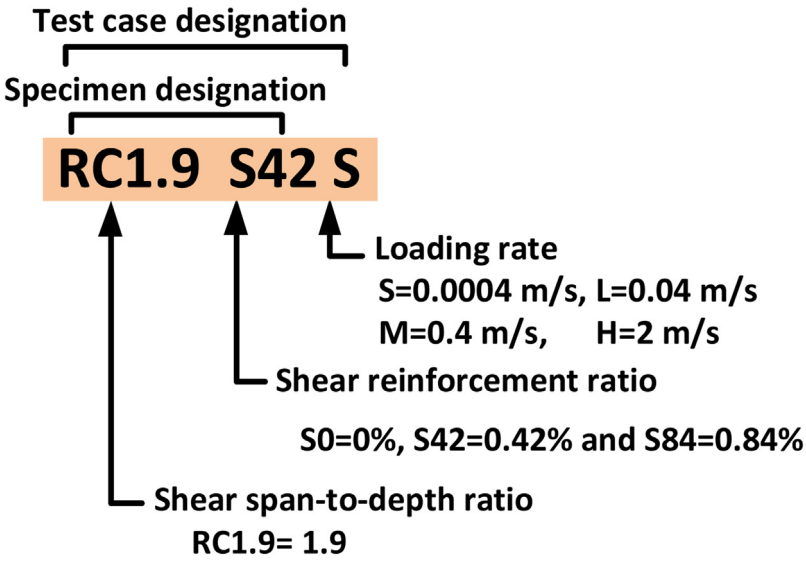

Fig. 9. Test case and specimen designations.

Table 1
The ultimate strength of tested beam specimens [4].

Specimen	Strain rates (1/s)	Dynamic shear resistance (kN)
RC1.9 S0	0.0059	170.1
	0.067	246.5
	0.59	290.5
	3.5	353.6
RC1.9 S42	0.0068	271.9
	0.041	300.6
	0.48	361.3
	3.1	417
RC1.9 S84	0.0027	331.8
	0.029	378.2
	0.46	420.75
	3.7	446.7

Table 2
Case study for prediction for $P_{Exp.}$ [4].

Specimen	Strain rates (1/s)	Dynamic shear resistance (kN)		Test/Predict
		Test	Predict	
RC1.9 S0	0.0059	170.1	286.81	0.59
	0.067	246.5	306.42	0.80
	0.59	290.5	334.35	0.87
	3.5	353.6	365.71	0.97
RC1.9 S42	0.0068	271.9	301.71	0.90
	0.041	300.6	318.25	0.94
	0.48#	361.3	352.05	1.03
	3.1	417	388.29	1.07
RC1.9 S84	0.0027	331.8	307.14	1.08
	0.029	378.2	328.33	1.15
	0.46	420.75	368.69	1.14
	3.7	446.7	413.47	1.08
			Mean	0.97
			SD	0.16
			C.O.V.	0.166

The coefficient of variation obtained from the results (0.176) displayed good accuracy and consistency for the values obtained. This was enough to consider the proposed STM model proper for assessment of the ultimate strength of RC deep beams under dynamic loading conditions, and different geometrical and material (steel and concrete strength) properties.

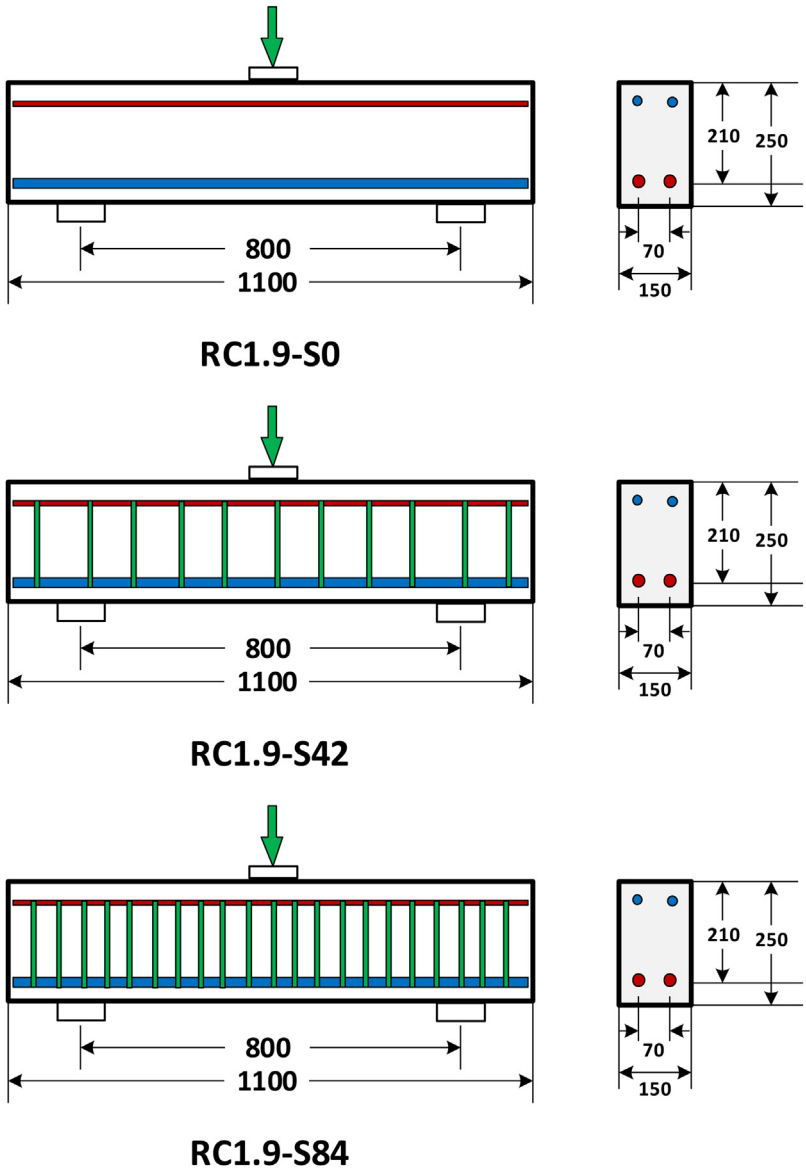

Fig. 10. Dimensions of RC deep beams and layout of reinforcements of the case study [4].

5. Parametric study

5.1. Numerical simulation case studies

After validating the proposed strut and tie model with the experimental results, this section displays a parametric examination to present more information about the behavior of RC deep beams under varying loading rates. Various key parameters such as shear span to effective depth ratios, longitudinal main reinforcement ratios, web reinforcement ratios and strain rates, used to study the response of deep beam specimens. Figs. 13 and 14 illustrate the effect of shear span to effective depth ratios and the longitudinal reinforcement ratios on the ultimate strength capacity of RC deep beams, in which there is a decreasing in the ultimate strength with increase of the shear span to depth ratio. The parametric study was simulated in the MATLAB/Simulink environment.

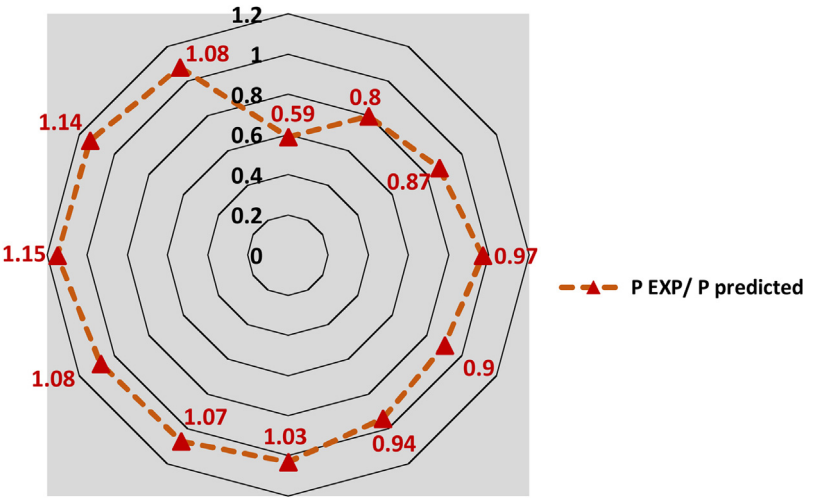

Fig. 11. Comparison between experimental and predicted ultimate strength.

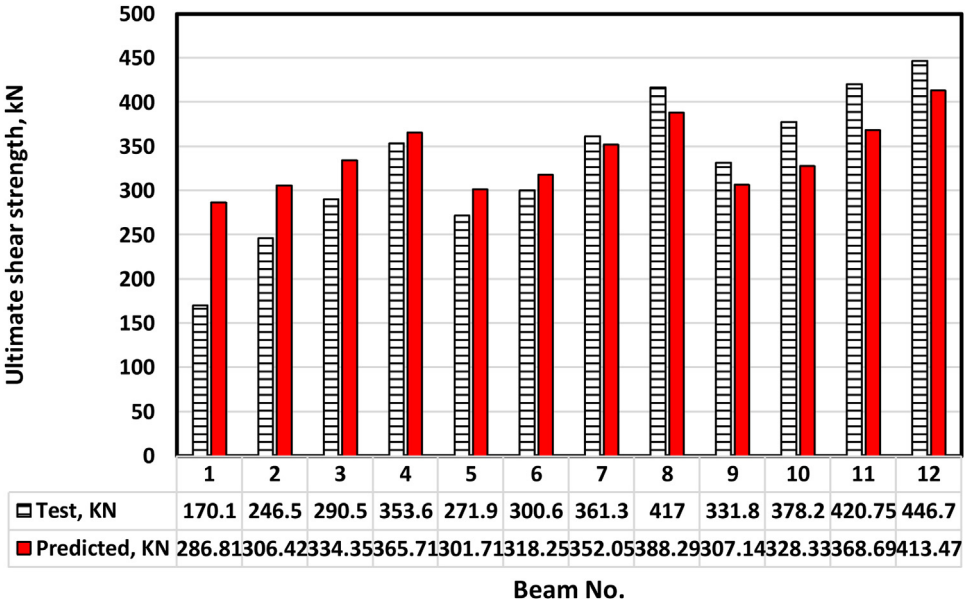

Fig. 12. Comparison between the predicted ultimate shear strength and the experimental.

5.2. Effect of main reinforcement ratio on DIF

A total of 36 experimental RC deep beams were examined to demonstrate the effect longitudinal reinforcement on DIF of maximum resistance under various strain rates, as shown in Fig. 15. Three span to effective depth ratios (a/d: 0.95, 1.43 and 1.9) were examined. As displayed in Fig. 15, there is a DIF increases with the increase of the flexural reinforcement ratio.

5.3. Effect of web reinforcement ratio on DIF

Fig. 11 displays the influence of web reinforcement on DIF of ultimate capacity of RC deep beam under various strain rates. From the results (Fig. 16), web reinforcement does not have a significant effect on DIF, but the important effect was on the ultimate strength of the RC deep beam. This is similar to an observation by Adhikary et al. [4].

5.4. Effect of shear span-to-effective depth ratio on DIF

In this case study, three span-to-effective depth ratios (a/d: 0.9, 1.43 and 1.9) were investigated. The changing in the ratio was for span length, whereas, the depth was kept constant for all specimens. Fig. 17 illustrates the influence of shear

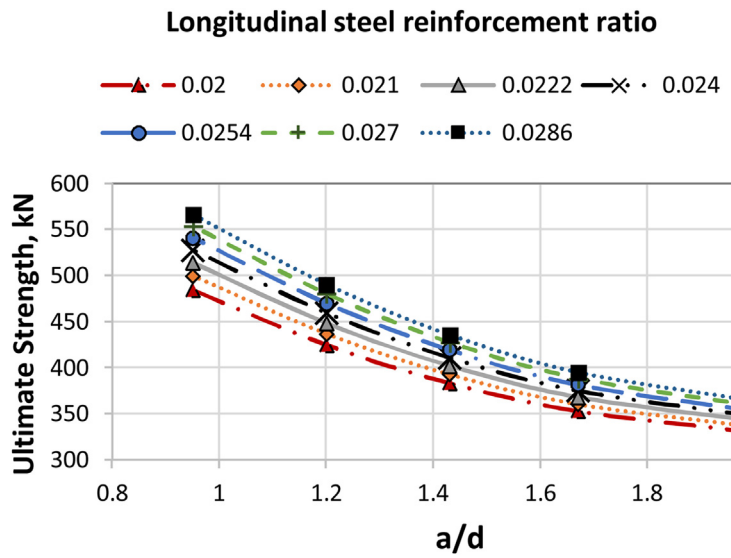

Fig. 13. Effect of shear span-to-effective depth ratio on ultimate strength of RC deep beams.

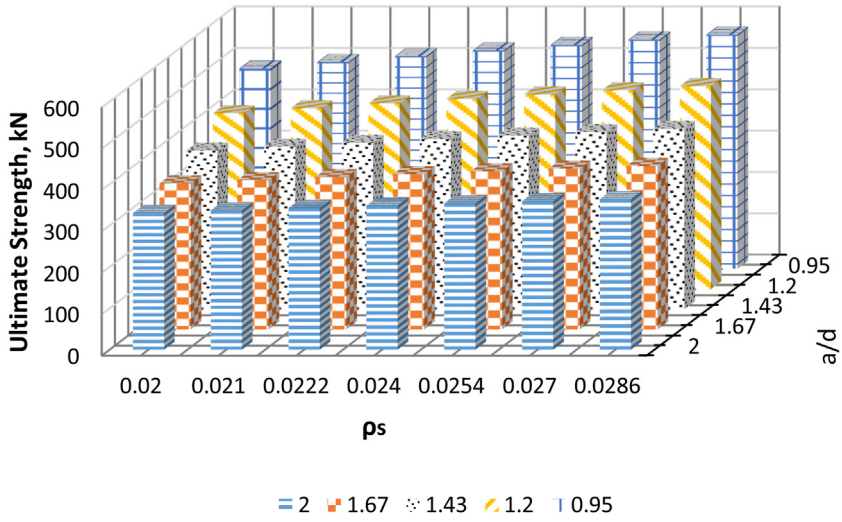

Fig. 14. Ultimate strength of RC deep beams with effect of different longitudinal reinforcement ratio and shear span-to-depth ratio.

span-to-depth ratio on the DIF of ultimate strength of the deep beam specimens. The results exhibit increasing in DIF with the increase of shear span-to-depth ratio of all strain rates.

6. Summary and conclusions

A simple STM approach is extended to account for the effect of strain rates, main reinforcement, and web reinforcement on the behavior of RC deep beams. Linear interactive failure is used to imply the softening effect. Moreover, the MATLAB SIMULINK software is used in simulating the proposed model. The experimental results [4] were compared with the predictions of proposed model A new effectiveness factor for concrete struts was proposed based on the failure principles of Mohr–Coulomb. The proposed STM exhibits efficiency in assessing dynamic shear resistance for RC deep beams under varying loading rates, which could be implemented quite satisfactorily. The main conclusions of the current study are presented below.

- The dynamic shear resistance of RC deep beams increases with loading rates increase.
- The analysis results indicated that the web reinforcement does not have significant effect on DIF of ultimate strength. Whereas, the results exhibit increasing in DIF with the increase of shear span-to-depth ratio for all strain rates.

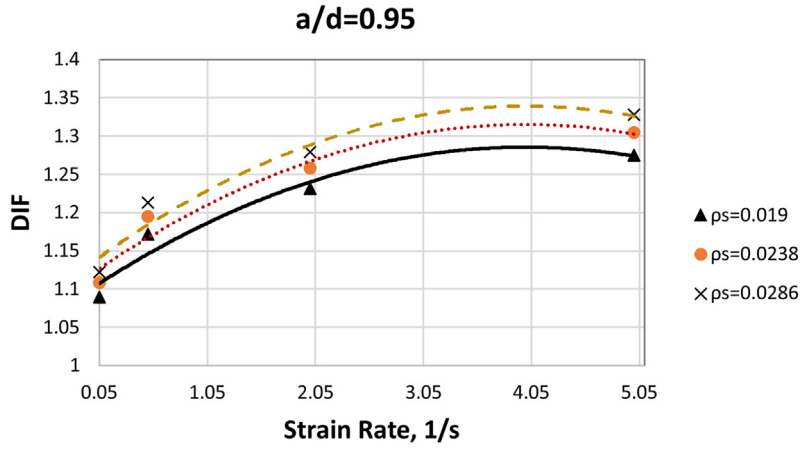

(a)

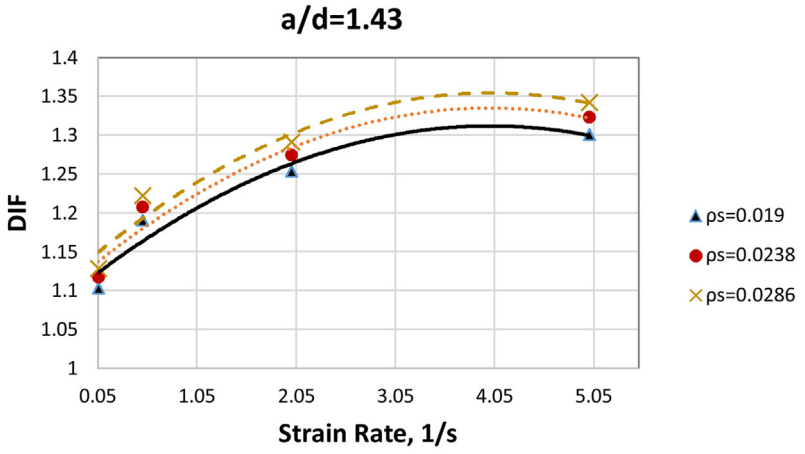

(b)

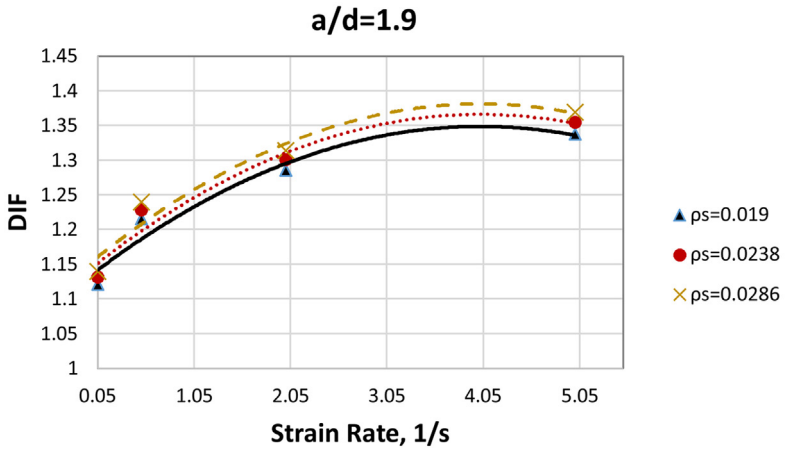

(c)

Fig. 15. Effect of longitudinal reinforcement ratios on DIF of ultimate shear resistance of RC deep beams: (a) a/d:0.95; (b) a/d:1.43; (c) a/d:1.9.

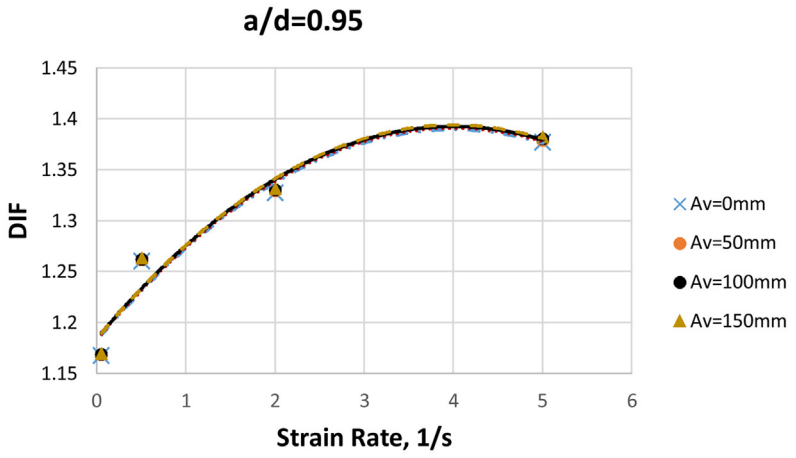

(a)

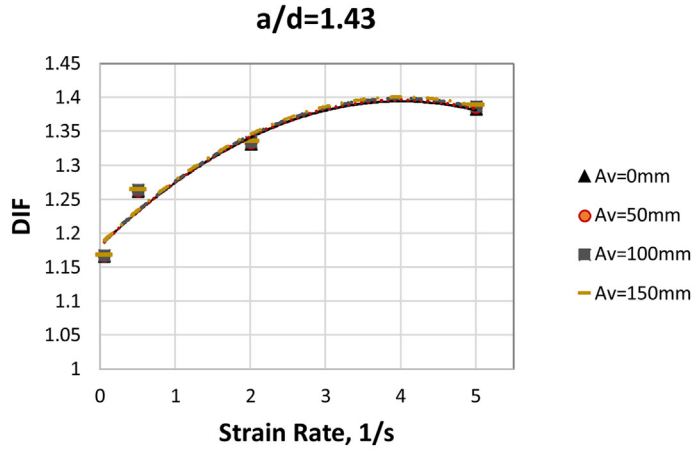

(b)

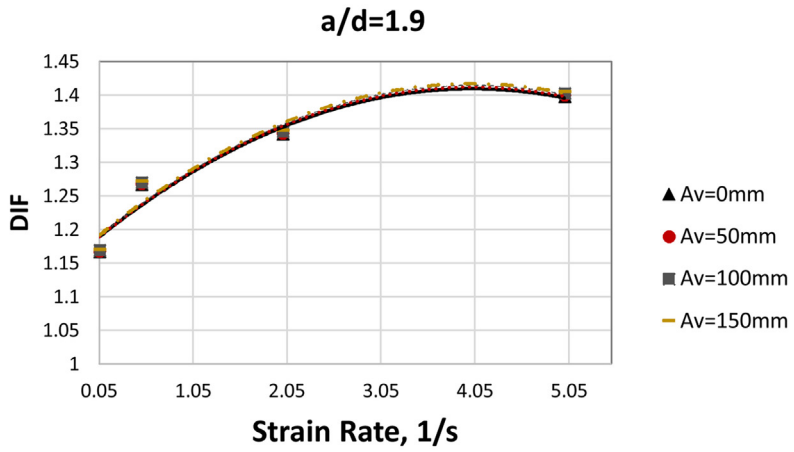

(c)

Fig. 16. Effect of transverse reinforcement on DIF of ultimate shear resistance of RC deep beams: (a) a/d:0.95; (b) a/d:1.43; (c) a/d:1.9.

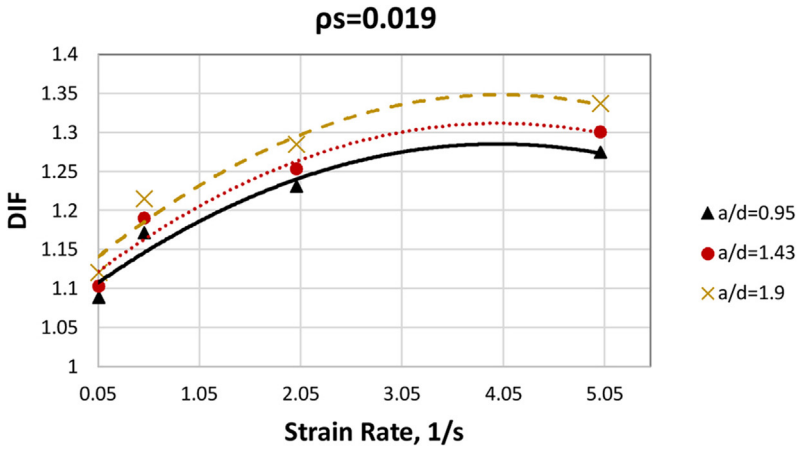

(a)

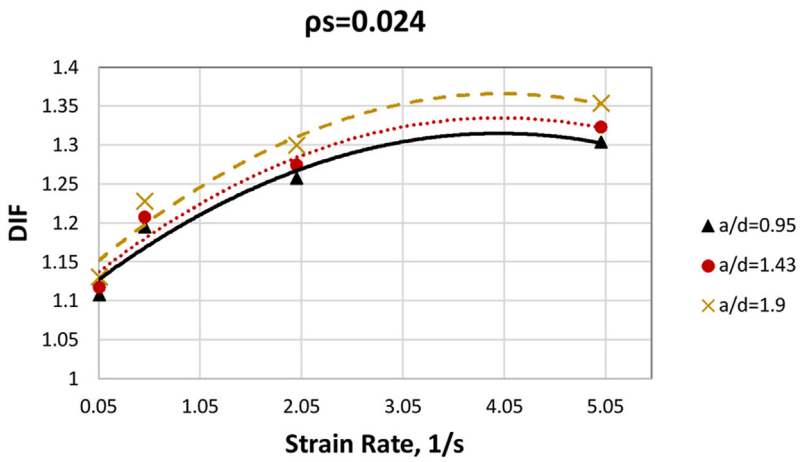

(b)

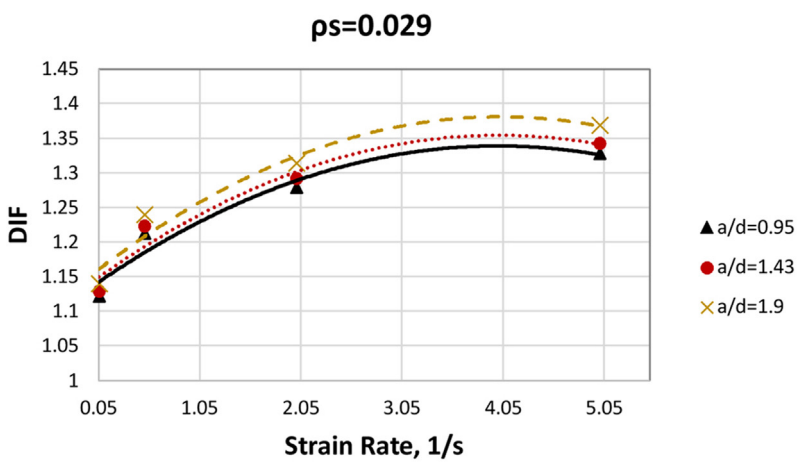

(c)

Fig. 17. Effect of shear span to effective depth ratios on DIF of ultimate shear resistance of RC deep beams: (a) rs:0.019; (b) rs:0.024; (c) rs:0.029.

- The comparison of results indicates that the proposed approach yields safe and appropriate estimates for RC deep beams with different strain rates.
- With mean 0.97, and coefficient of variation of 0.166, the proposed effectiveness factor for concrete struts was indicated an ability to provide a highly accurate estimation of the ultimate shear strength of deep beams subjected to dynamic loads. The new effectiveness factor proposed can be used as a guide line in the design process of STM under dynamic loads.
- For increasing strain rates values, the ultimate shear strength predicted increases slowly with stress distribution factor, k increasing.

Acknowledgements

The authors would like to express their gratitude to the support provided by the Universiti Putra Malaysia (UPM). The first author also acknowledges a scholarship program from the Ministry of Higher Education, Iraq.

. A.1 Worked Example

The following example show the calculation involved in determining V_n for RC deep beams under loading rates effect.

. Example RC de lates effect [4]

T ultimate capacity of Beam (Rc1.9 S42) in Table 2 is to be calculated based. The geometrical properties of the beam are: a = 400mm, d = 210mm, h = 250mm, b_w = 150mm, l_b = 50mm; concrete strength: $f'c$ = 40MPa; flexural reinforcement: A_s = 760mm^2, f_y = 371MPa; transverse reinforcement: A_h = 0mm^2, f_{yh} = 342MPa; A_v = 126mm^2, f_{yv} = 342MPa, strain rate = 0.48s^{-1}.

Answer:

$$l_a = 2(h - d) = 2(250 - 210) = 80mm$$

$$lc = 57.839mm\,(fromtheiteration)$$

$$\tan\theta_s = \frac{h - \frac{l_a}{2} - \frac{l_c}{2}}{a} \cong \frac{250 - \frac{80}{2} - \frac{57.839}{2}}{400} \cong 0.4553$$

$$\therefore \sin\theta_s = 0.4273, \text{ and } \cos\theta_s = 0.9101$$

$$f'_{C,dyn} = f_{\acute{c}}\left(\frac{\dot{\varepsilon}}{\dot{\varepsilon}_s}\right)^{0.006\left[\log 10\left(\frac{\dot{\varepsilon}}{\dot{\varepsilon}_s}\right)\right]^{1.05}} = 40\left(\frac{0.48}{1.2\times10^{-5}}\right)^{0.006\left[\log 10\left(\frac{0.48}{1.2\times10^{-5}}\right)\right]^{1.05}} = 54.386MPa$$

$$f_{y,dyn} = f_y(1.202 + 0.04\log 10\dot{\varepsilon}) = 371\times(1.202 + 0.04\log 10(0.48)) = 441.212MPa$$

$$f_{yv,dyn} = f_y(1.202 + 0.04\log 10\dot{\varepsilon}) = 342\times(1.202 + 0.04\log 10(0.4)) = 406.723MPa$$

$$A_{str} = 150(80\times0.91 + 50\times0.4273) = 14025mm^2$$

$$A_c = b_w h = 37500mm^2$$

$$f_{ct} = 0.5\sqrt{54.386} = 3.9347N/mm^2$$

$$f_t = \frac{kA_s f_{y,dyn}\sin\theta_s}{A_c/\sin\theta_s} + \frac{2A_w f_{yw,dyn}\sin\left(\theta_s+\theta_w\right)}{A_c/\sin\theta_s}\frac{d_w}{d} + f_{ct} = 8.3125MPa$$

$$V_n = \upsilon A_{str}\acute{f}_{c,dyn}\sin\theta_s = \left(1 - \frac{kT_s\sin^2\theta_s}{A_c f_t}\right)A_{str}\acute{f}_{c,dyn}\sin\theta_s = 176.037kN$$

$$P_u = 2\times V_n = 2\times176.037 = 352.0474kN$$

In this worked example, the Ultimate capacity P_{Exp} from experiment is 361.3 kN [4]. Thus, the ratio of P_u/P_{exp} is 1.03.

References

[1] AASHTOL, Bridge Design Specifications, Customary US Units, with 2008 Interim Revisions, American Association of State Highway and Transportation Officials, Washington, DC, 2008.
[2] ACI318-11, Building Code Requirements for Structural Concrete ACI 318 -11and Commentary 318R -11: ACI 318-08/318R-11, American Concrete Institute, Farmington Hills (MI, USA), 2011.
[3] S.D. Adhikary, B. Li, K. Fujikake, Dynamic behavior of reinforced concrete beams under varying rates of concentrated loading, Int. J. Impact Eng. 47 (2012) 24–38, http://dx.doi.org/10.1016/j.ijimpeng.2012.02.001.
[4] S.D. Adhikary, B. Li, K. Fujikake, Strength and behavior in shear of reinforced concrete deep beams under dynamic loading conditions, Nucl. Eng. Des. 259 (2013) 14–28, http://dx.doi.org/10.1016/j.nucengdes.2013.02.016.
[5] R. AL-Mahaidi, Wenchuan post-earthquake reconstruction by utilizing composite tubular construction and FRP retrofitting technology, J. Sichuan Univ. (Eng. Sci. Ed.) 41 (3) (2009).
[6] ASCE-ACI445, Recent approaches to shear design of structural concrete, J. Struct. Eng. 124 (12) (1998) 1374.
[7] A. Belarbi, T.T. Hsu, Constitutive laws of softened concrete in biaxial tension compression, ACI Struct. J. 92 (5) (1995).
[8] CEB-FIP, CEB-FIP Model Code 1990: Design Code, Comité euro-international du béton, Telford, 1993.
[9] R.D. Cook, W.C. Young, Advanced Mechanics of Materials, vol. 2, Prentice Hall Upper Saddle River, NJ, 1999.
[10] CSA-S806-02, Design of Concrete Structures, Canadian Standards Association: Mississauga, Canadian Standard Association, Ont, 2004.
[11] J.-f. Dong, Q.-y. Wang, Y.-m. Zhu, C.-c. Qiu, Experimental study on RC beams strengthened with externally bonded FRP sheets [J], J. Sichuan Univ. (Eng. Sci. Ed.) 5 (2010) 030.
[12] D. Duthinh, Sensitivity of shear strength of reinforced concrete and prestressed concrete beams to shear friction and concrete softening according to modified compression field theory, ACI Struct. J. 96 (4) (1999).
[13] EC2, Eurocode 2: Design of Concrete Structures: Part 1-1: General Rules and Rules for Buildings, British Standards Institution, 2004.
[14] T. El Maaddawy, S. Sherif, FRP composites for shear strengthening of reinforced concrete deep beams with openings, Compos. Struct. 89 (1) (2009) 60–69, http://dx.doi.org/10.1016/j.compstruct.2008.06.022.
[15] S.J. Foster, A.R. Malik, Evaluation of efficiency factor models used in strut-and-tie modeling of nonflexural members, J. Struct. Eng. 128 (5) (2002) 569–577, http://dx.doi.org/10.1061/(ASCE)0733-94452002128:5(569).
[16] K. Fujikake, B. Li, S. Soeun, Impact response of reinforced concrete beam and its analytical evaluation? J. Struct. Eng. 135 (8) (2009) 938–950.
[17] S.M. Kulkarni, S.P. Shah, Response of reinforced concrete beams at high strain rates, ACI Struct. J. 95 (6) (1998).
[18] I.-J. Lin, S.-J. Hwang, W.-Y. Lu, J.-T. Tsai, Shear strength of reinforced concrete dapped-end beams, Struct. Eng. Mech. 16 (3) (2003) 275–294, http://dx.doi.org/10.12989/sem.2003.16.3.275.
[19] W.-Y. Lu, I.-J. Lin, Behavior of reinforced concrete corbels, Struct. Eng Mech. 33 (3) (2009) 357–371.
[20] J.G. MacGregor, J.K. Wight, S. Teng, P. Irawan, Reinforced Concrete: Mechanics and Design, vol. 3, Prentice Hall Upper Saddle River, NJ, 1997.
[21] Mutsuyoshi, H., and Machida, A., (1984). Properties and failure of reinforced concrete members subjected to dynamic loading (vol. 6, pp. 521–528): ransactions of the Japan Concrete Institute.
[22] B. Riisgaard, T. Ngo, P. Mendis, C. Georgakis, H. Stang, Dynamic increase factors for high performance concrete in compression using split hopkinson pressure bar, Paper Presented at the 6th International Conference on Fracture Mechanics of Concrete and Concrete Structures (2007).
[23] S. Saatci, F.J. Vecchio, Nonlinear finite element modeling of reinforced concrete structures under impact loads, ACI Struct. J. 106 (5) (2009) 717.
[24] K. Tan, K. Tong, C. Tang, Direct strut-and-tie model for prestressed deep beams, J. Struct. Eng. 127 (9) (2001) 1076–1084.
[25] Tong, K., (1997). Strut-and-Tie Approach to Shear Strength Prediction of Deep Beams (MEng Thesis). Singapore: Nanyang Technological University.
[26] F.J. Vecchio, M.P. Collins, The modified compression-field theory for reinforced concrete elements subjected to shear, ACI J. Proc. (1986).
[27] F.J. Vecchio, M.P. Collins, Compression response of cracked reinforced concrete, J. Struct. Eng. 119 (12) (1993) 3590–3610.
[28] W. Wang, S. Wu, H. Dai, Fatigue behavior and life prediction of carbon fiber reinforced concrete under cyclic flexural loading? Mater. Sci. Eng.: A 434 (1) (2006) 347–351.
[29] Zeng, L.H., and Tan, K.H, (1999). Singapore Patent No.: N.T.U. National Undergraduate Research Project.